Exosomal miR-185 inhibits esophageal squamous cell carcinoma progression and predicts prognosis

（エクソソーム中 miR-185 は食道扁平上皮癌の進展を阻害し予後を予測する）

千葉大学大学院医学薬学府
先端医学薬学専攻
（主任：松原久裕 教授）
Abula　Maiyulan

Introduction

Esophageal cancer is the eighth most common malignant neoplasm and the sixth leading cause of cancer-related deaths worldwide (1). Despite advances in esophageal cancer treatment over recent decades, patient prognosis has improved little (2). Even with the introduction of combination treatment regimens and early diagnostic technology, the survival rate remains unsatisfactory, with an approximately 17%–20% 5-year overall survival rate (3). Lymph node (LN) metastasis is one of the most important prognostic factors and generally indicates a poor outcome (4). Therefore, the identification of new prognostic biomarkers and the development of effective treatment methods are imperative for improving the clinical outcomes of patients with ESCC.

Exosomes are a class of extracellular vesicles; that is, lipid bilayer-enclosed carriers of proteins, nucleic acids, lipids, and metabolites, which are secreted by cells into the extracellular environment (5). As such, exosomes can transfer bioactive molecules from donor to recipient cells and influence their biological activities (6). Tumor-derived exosomes are released into peripheral blood, and their quantity is a prognostic marker of ESCC (7). Furthermore, tumor-derived exosomes have been shown to alter cellular gene expression and contribute to tumor progression in ESCC (8). Therefore, a comprehensive understanding of the mechanisms through which circulating miRNAs influence cancer progression is warranted.

Emerging evidence suggests that hypoxia contributes to ESCC resistance against first-line chemotherapy, such as cisplatin and 5-fluorouracil [5-FU] (9). Our laboratory previously reported that HIF-1α plays an essential role in hypoxia-induced ESCC progression by maintaining crucial mechanisms, such as epithelial–mesenchymal transition (EMT), proliferation, migration/invasion, apoptosis, cell cycle arrest, and chemoresistance, influencing patient prognosis (10). However, the mechanisms through which hypoxia influences miRNAs in ESCC remain poorly understood.

MicroRNAs (miRNAs) are small noncoding RNAs that regulate gene expression at the post-transcriptional level (11). A growing body of evidence has demonstrated that miRNAs are implicated in the initiation and progression of ESCC by regulating the expression of

oncogenes and tumor suppressors (12). The prognostic applications of miRNAs in ESCC have recently attracted interest. miR-185 has been identified as a tumor-suppressive miRNA in multiple types of cancers, including hepatocellular carcinoma (13), osteosarcoma (14), and prostate cancer (15), in addition to being associated with the prognosis of colon (16) and gastric cancer (17). However, there is limited literature on the role of exosomal miR-185 in ESCC. The roles of miR-185 in the metastasis, locoregional staging, and molecular mechanisms of ESCC and survival of ESCC patients have been reported (18-20); however, in the present study, we observed the alteration of exosomal miR-185 expression under hypoxia conditions, its connection with lymph node metastasis before chemotherapy, and accordingly, the sensitivity of ESCC cells to chemotherapy. Moreover, we investigated the association of exosomal miR-185 levels with clinicopathologic factors and prognosis in ESCC, and explored the mechanism underlying the role of exosomal miR-185 via *in vitro* experiments using ESCC cell lines and bioinformatics analyses. Our findings highlight the importance of exosomal miR-185 as a prognostic biomarker and therapeutic target in ESCC.

Materials and methods

Clinical samples

Plasma samples were collected from 89 patients diagnosed with esophageal cancer at Chiba University Hospital (Chiba, Japan) between May 2011 and April 2017. Patients aged 20-85 years with histologically diagnosed esophageal squamous cell carcinoma were included, patients with other cancers were excluded, but no other exclusion criteria such as history of other medical diseases were defined. Written informed consent was obtained from all participants. This study was approved by the Ethics Committee of the Graduate School of Medicine, Chiba University (approval number: 1264). Blood examination and sampling were performed before treatment. After receiving patient plasma samples, we centrifuged these at 4°C and 3000 rpm for 10 min, storing them at −80°C.

Cell lines and cell culture

The KYSE-960 esophageal cancer cell line was purchased from JCRB Cell Bank, and the T.Tn cell line was provided by the Cell Resource Center at Tohoku University, Japan. The cells were cultured in Dulbecco's modified Eagle's medium (DMEM; Life Technologies, Grand Island, NY, USA) supplemented with 10% fetal bovine serum (FBS) and 100 U/ml penicillin maintained at 37°C in a humidified atmosphere containing 5% CO_2. For exosome isolation under normoxic conditions, cells were incubated in DMEM replenished with 10% exosome-free FBS and 1% penicillin/streptomycin at 37 °C, 21% O_2, and 5% CO_2 for 48 h. For physical hypoxia conditions, cells were incubated at 1% O_2 and 5% CO_2 in a multi-gas incubator for 48 h (#BL-43MD, TOSC, Japan).

Profiling of exosomal miRNAs extracted from normoxia/hypoxia culture medium

Microarray analysis was performed on the total RNA extracted from exosomes isolated by ultracentrifuge at 10,000 × *g* and 4°C for 90 min (Optima TLX Ultracentrifuge, Beckman Coulter, CA, USA), as previously reported (8). Cells were cultured to 80% confluence. From normoxic and hypoxic KYSE-960 and T.Tn cell culture medium, using Affymetrix GeneChip miRNA 4.0 according to the manufacturer's protocol. Exosome extraction was confirmed by transmission electron microscopy and nanoparticle tracking analysis. Chip data analysis was performed using the R software.

Exosome isolation from plasma

Each plasma sample (1–1.5 ml) was centrifuged at 2,000 × *g* for 20 min at room temperature to remove cells and debris. Exosomes were isolated using the total exosome isolation kit (from plasma) [Invitrogen, catalog number: 4484450], according to the manufacturer's instructions and it is the same method that was used in our previous report (7).

Exosome isolation from the cell culture medium

A total of 5×10^6 cells were incubated in medium with 10% exosome-free FBS for 48 h and total (10 ml) cell culture medium was harvested. Exosomes were isolated using the total exosome isolation kit (from cell culture medium) [Invitrogen, catalog number: 4478359], according to manufacturer's instructions and it is the same approach that was used in our previous report (7).

Transmission electron microscopy (TEM)

TEM was performed using a carbon-coated copper grid (200 mesh), and staining was performed using a 2% phosphotungstic acid solution (pH, 7.0–7.4). The samples were observed under a transmission electron microscope (H-7650; Hitachi High-Technologies Corporation, Tokyo, Japan) at an acceleration voltage of 80.0 kV.

MiRNA and mRNA isolation and detection via quantitative real-time polymerase chain reaction (qRT–PCR)

Total RNA was extracted from the exosomes using the Total Exosome RNA and Protein Isolation Kit (Invitrogen), according to the manufacturer's protocol. Total cellular RNA was extracted using the Mini Kit (QIAGEN, Hilden, Germany), according to the manufacturer's protocol. Total RNA was reverse-transcribed to cDNA using a High-Capacity RNA-to-DNA^{TM} Kit (Thermo Fisher Scientific), according to the manufacturer's protocol. qRT–PCR analysis was performed using the SsoFast^{TM} EvaGreen Supermix (Bio-Rad). MiR-16, U6 small nuclear RNA and β-actin gene were used as internal references for exosomal miR-185 and BCL-2 expression, respectively. Relative gene expression was calculated using the $2^{-\Delta\Delta Cq}$ method; BCL-2 and miR-185 specific primers are detailed in Supplementary Table S1.

MiRNA transfection

Cells were seeded in six-well plates (2.5×10^5 cells per well) and transfected with miR-185 mimic or negative control using Lipofectamine™ RNAiMAX Transfection Reagent (Invitrogen). Mimic and negative control miR-185 were purchased from Thermo Fisher Scientific (Catalog number: 4427975). The miR-185 mimic and negative control were transfected into cells for 48 h.

Migration, invasion, cell proliferation, and colony formation assays

Migration and invasion abilities were detected using Transwell assays. In a 24-well plate, 5×10^4 transfected cells were seeded in the upper chamber (Corning Matrigel Invasion Chamber, BD Biosciences, San Jose, CA, USA) in FBS-free medium. A medium containing 10% FBS was added to the lower chamber. After incubation for 48 h, non-invading cells were removed from the upper chamber with a cotton swab, whereas cells on the lower surface were fixed and stained using Diff-Quick Staining (Sysmex Corp, Yokohama, Japan). Images of three random fields from triplicate wells were recorded. Migration assays were performed in the same manner, except that the chambers had no Matrigel coating, and the incubation time was 24 h. A total of 5×10^3 (cells/well) transfected cells (KYSE-960, T.Tn) were placed in a 96-well plate. Cell proliferation was assessed using a Cell Counting Kit-8 (CCK-8; Dojindo, Kumamoto, Japan) every 24 h. For the colony formation assay, 800 cells/well were plated in a 6-well plate and maintained in complete culture medium. After 2 weeks, the colonies were fixed with a Differential Quick III Stain Kit (International Reagents, Kobe, Japan) for 15 s. Visible colonies were photographed and manually counted.

Apoptosis and cell cycle analyses

ESCC cells were treated with cisplatin (at the IC50) for 48 h. The cells were harvested and washed with PBS, resuspended with 100 μL Annexin V Binding Solution, and incubated with 5 μL Annexin V FITC and 5 μL PI solution (Annexin V-FITC Apoptosis Detection Kit; Nacalai Tesque, Kyoto, Japan) at room temperature for 15 min. Finally, 400 μL of Annexin V Binding Solution was added prior to analysis. The results were

analyzed using the FlowJo software (TreeStar, Ashland, Oregon, United States). BCL-2 expression was quantified by qRT–PCR using beta actin as a control.

For cell cycle analysis, cells were harvested after 48 h of transfection, washed with PBS, harvested, and fixed with pre-cooled 70% ethanol at 4°C for at least 24 h. After washing, the cells were incubated with 100 μg/mL RNaseA (Invitrogen Carlsbad, USA) and 0.1% Triton-100 at 37°C for 5 min and then stained with 50 μg/mL PI at room temperature for 30 min in the dark. The DNA content was measured using the MOdfitLT software program (BD Biosciences, CA, USA).

Gene set enrichment analyses (GSEA)

Enrichment analysis of The Cancer Genome Atlas (TCGA) data (https://www.cbioportal.org/datasets) was performed using GSEA v4.0.1. A total of 195 RNA-seq and miRNA-seq datasets from patients with esophageal cancer were used to evaluate miRNA expression. Patients were divided into miR-185-5p-high and -low expression group based on median miR-185-5p expression.

Statistical analysis

Statistical analysis was performed using SPSS21 (SPSS, Chicago, IL, USA) and GraphPad Prism 7.04 (GraphPad Software, Inc., La Jolla, CA, USA). Student's t-test and one-way analysis of variance (ANOVA) with Tukey's as a post hoc test were employed for quantitative variables, and a chi-square test and Fisher's exact test were employed for qualitative variables to compare the characteristics of each group. Survival curves were plotted using the Kaplan–Meier method. Results were compared using the log-rank test. Statistical significance was considered when $p < 0.05$.

Results

MiRNA array expression analysis in KYSE-960 and T.Tn cells culture medium

miRNA array analysis was performed to screen differentially expressed exosomal miRNAs in KYSE-960 and T.Tn cells culture medium under normoxia and hypoxia conditions. The expression of 33 exosomal miRNAs exhibited two-fold downregulation, whereas 12 miRNAs exhibited two-fold upregulation in normoxic vs. hypoxic KYSE-960 cells. In the T.Tn cell line, 33 exosomal miRNAs were downregulated two-fold, and nine were upregulated two-fold. Cluster analysis of the intersecting miRNAs is shown in Fig. 1A. The expression level of exosomal miR-185 decreased in both KYSE-960 and T.Tn cell culture medium under hypoxic conditions (fold change relative to that in KYSE-960 cells: 0.32, T.Tn fold change: 0.22; Fig. 1B). Different cells respond differently to external stimuli, which may be why inconsistent fold changes occur in the expression levels of miRNAs in KYES-960 and T.Tn cell lines.

Analysis of MiR-185-5p expression in ESCC cells and exosomes

MiR-185-5p expression in ESCC cells (T.Tn and KYSE-960) was slightly higher than that in normal esophageal keratinocytes (R2C3), although the difference was not significant (Supplementary Fig. S1). MiR-185-5p expression in exosome derived from T.Tn cell culture medium was twice as more than normal esophageal keratinocytes, but the difference was not statistically significant (T.Tn vs. R2C3, $p = 0.0750$). Meanwhile, the miR-185-5p expression in exosomes derived from KYSE-960 culture medium was significantly higher than that in normal esophageal keratinocytes (KYSE-960 vs. R2C3, $^{**}p = 0.0036$; Fig. 2A).Correlation analysis of miR-185 expression in R2C3, T.Tn, TE1,

TE6, TE11, TE14, KYSE-960, KYSE-410, and SCCVII cells and exosomes was conducted via qRT–PCR ($r^2 = 0.6743$, $p = 0.0464$; Fig. 2B).

MiR-185 overexpression suppresses the invasion, migration, and colony formation abilities of esophageal cancer cells *in vitro*

The overexpression of miR-185 in KYSE-960 and T.Tn cells was confirmed via qRT–PCR after miR-185 transfection (Supplementary Fig. S2). The invasion and migration abilities of miR-185-overexpressing cells decreased significantly compared with those of the negative controls (invasion: KYSE-960, miR-185 vs. control, ***p = 0.0001; T.Tn, miR-185 vs. control, ***p = 0.0022 [Fig. 3A]; migration: KYSE-960, miR-185 vs. control, ***p = 0.0003; T.Tn, miR-185 vs. control, **p = 0.0034 [Fig. 3B]). Cells transfected with miR-185 showed a lower survival rate than those in the negative control group, as determined via colony formation assays (KYSE-960, miR-185 vs. negative control, ***p = 0.0005; T.Tn, miR-185 vs. negative control, *p = 0.01 [Fig. 3C]). The cell growth curve was significantly slower after miR-185 transfection than that in the control KYSE-960 cells (**p = 0.002). The cell growth curve of miR-185-transfected T.Tn cells was slower than that of controls (p = 0.6) [Fig. 3D, Supplementary Fig. S3].

MiR-185 regulates cell apoptosis after cisplatin treatment and cell cycle progression *in vitro*

The apoptosis rate of miR-185-transfected KYSE-960 and T.Tn cells after cisplatin exposure for 48 h was significantly higher than that of negative control cells. The apoptosis rate of miR-185-transfected KYSE-960 and T.Tn cells after cisplatin treatment was significantly higher than that in the negative control group (KYSE-960 mimic vs.

control, *p = 0.027; T.Tn mimic vs. control, ***p = 0.0001; Fig. 4A). In addition, BCL-2 mRNA expression levels were reduced in both the KYSE-960 and T.Tn mimic groups (Fig. 4B). Cell cycle analyses showed that the percentages of ESCC cells in the G0/G1 phase after miR-185 transfection was significantly higher than that in control cells, while the percentage of ESCC cells in the G2/M phase was significantly lower (KYSE-960 G0/G1,*p < 0.05, S/G2M,*p < 0.02; T.Tn G0/G1,*p < 0.04, S/G2M,*p < 0.03; Fig. 4C, Supplementary Fig. S4)

MiR-185-5p-associated signaling

Publicly available TCGA expression data from patients were divided into miR-185-high and -low expression groups based on median miR-185 expression. Thereafter, GSEA was performed. The high miR-185 expression group was enriched in signaling pathways, such as cell death (apoptosis) and DNA damage (UV Response Up, reactive oxygen species, oxidative phosphorylation) and p53 signaling in the T.Tn cell line (Fig. 5A–E).

Characterization of exosomes from patient samples

We isolated exosomes from the plasma samples of 89 patients with ESCC. To confirm the successful isolation of exosomes, we employed TEM to characterize their shape in the supernatant (Supplementary Fig. S5). Plasma exosomes exhibited elliptical shapes.

Relationship between circulating miR-185 levels and clinicopathological characteristics of patients with ESCC

The clinicopathological characteristics of patients are summarized in Table 1. The total number of patients was 89, including nine endoscopically treated cases, 55 preoperatively

untreated surgical cases, and 25 cases treated via neoadjuvant chemotherapy, followed by surgery. Pre-treatment staging is performed by whole body search including PET/CT. Patients were divided into circulating miR-185-high (n = 28) and -low (n = 61) groups. A cutoff value of 4.3 was set for the miR-185/miR-16 ratio based on the mean value of miR-185 in esophageal cancer patients. In patients with high circulating exosomal miR-185, the frequency of lymph node metastasis in the preoperative diagnosis was significantly lower (cN category, **p = 0.0045), as was the cStage (cStage category, ***p = 0.0001).

Although the sample size was small, the preoperative patient group with high circulating exosomal miR-185 tended to exhibit a slightly higher response rate to chemotherapy than patients with low circulating exosomal miR-185, but not statistically significant. (p = 0.081, Table 2).

Progression-free survival (PFS) and disease-specific survival (DSS) of ESCC patients after initial treatment

The 5-year PFS rate in the exosomal miR-185-high group was 92.1% (95% CI 82.0%–103%), which was significantly higher (p = 0.030, log-rank test) than that in the exosomal miR-185-low group (66.9%, 95% CI 54.0%–80.0%). The 5-year DSS rate in the exosomal miR-185-high group was 100%, which was significantly higher (p = 0.020, log-rank test) than that in the exosomal miR-185-low group (76.5%, 95% CI 64.0%–89.0%; Fig. 6).

Discussion

ESCC is one of the most lethal cancers and a public health issue of great concern worldwide (21). Despite advances in its diagnosis and treatment, patient survival rates remain unsatisfactory (22). Therefore, identification of novel biomarkers and therapeutic targets in ESCC is urgently needed.

Exosomal miRNAs can be easily isolated from peripheral blood, which makes them candidate noninvasive biomarkers (23). Their potential to serve as biomarkers in patients with ESCC has been previously reported, along with a possible mechanism of exosomal trafficking (24). Exosomes influence gene expression, and thus, various biological processes (25). However, the influence of exosomal miRNA-185 levels in plasma on cancer treatment outcomes has been poorly investigated. It has been reported that plasma miR-185 levels are decreased in patients with ESCC and that tumor metastasis is suppressed by targeting RAGE (20). The impact of differential storage conditions and differential treatment on the stability and abundance of individual and total miRNAs in human plasma and plasma exosomes have been investigated; it has been highlighted that exosomal miRNAs have the potential to serve as biomarkers based on their stability under various conditions compared with plasma miRNAs (26). Thus, there is a possibility that exosomal miRNAs could serve as novel therapeutic targets for the development of effective methods for ESCC treatment. However, this study is the first to determine the different profiles of circulating exosomal miR-185 levels in patients with ESCC. We found that exosomal miR-185 is associated with lymph node-metastasis and may act as a predictor of the prognosis of ESCC patients. The data from the current study suggest that exosomal miR-185 is important for esophageal cancer initiation and progression and holds promise as a novel metastasis suppressor in esophageal cancer.

Hypoxia enhances the degree of glycolysis, angiogenesis, other survival responses in tumors, as well as their invasion and metastasis abilities, by activating relevant gene expression through hypoxia-inducible factors (HIFs) (27). The expression level of HIF-1α is elevated in cancer cell lines under hypoxia and drives oncogenic expression in ESCC, being associated with a poor prognosis (10). In our study, the expression of 33 exosomal miRNAs was downregulated in both KYSE-960 and T.Tn cell culture medium under hypoxia, whereas certain exosomal miRNAs were upregulated. Importantly, exosomal miR-185 expression decreased under hypoxia in both cell line culture medium. MiRNA dysregulation plays a critical role in the initiation and progression of multiple human cancers (28, 29), by either promoting (30) or suppressing tumorigenesis (31). The characterization of miRNAs involved in ESCC progression and their targets may contribute to the identification of new prognostic markers and therapeutic targets (32). Circulating miRNAs have recently emerged as potential biomarkers for various cancers (33). In the present study, exosomal miR-185 was significantly associated with cN and cStage categories, with high exosomal miR-185 levels in plasma being associated with a good prognosis in ESCC patients. Overexpressed miR-185 plays a suppressive role in tumor malignancy, paving the way for the development of effective treatment methods in ESCC.

MiRNAs are associated with lymph node metastasis in esophageal cancer (28, 29, 34), which may provide new insight for designing better therapeutic strategies. Furthermore, albeit based on a limited number of cases, our findings indicated that circulating miR-185 might not be able to influence chemotherapy sensitivity but predict lymph node metastasis prior to chemotherapy (Table 2). To provide new insights for designing better therapeutic strategies to treat esophageal cancer in patients with lymph node-metastasis

and to predict prognosis more accurately, further study in a larger cohort and a detailed mechanistic investigation are warranted.

Overcoming cisplatin resistance is a major goal in cancer therapy. One of the most widely accepted approaches is through combination with other agents that enhance cisplatin toxicity(35). In this study, overexpression of miR-185 regulated cancer cell cycle progression and induced apoptosis after cisplatin treatment. Apoptosis rate is around 10% without any other intervention except for miR-185 transfection in human gastric cancer cell line (36). In the other article, the apoptosis rate is around 20% without any other intervention except for miR-185 transfection in breast cancer cell line(37). But in our study, negative control of ESCC cell lines with the intervention of CDDP for 48 h and the target group was with the intervention of miR-185 transfection and CDDP. So, at this point, considering the previously reported numbers, it is somewhat reasonable that apoptosis rate is higher than 10%. Tumor cells may utilize several molecular mechanisms to suppress apoptosis and acquire resistance to cytotoxic agents, such as via upregulation of the antiapoptotic protein BCL-2 (38). In the present study, BCL-2 mRNA levels were suppressed in miR-185-overexpressing cells.

Furthermore, we observed a significant enrichment for HALLMARK gene sets related to cell death (apoptosis), DNA damage (UV Response Up, reactive oxygen species, and oxidative phosphorylation), and p53 in patients with high vs. low miR-185 expression. Such dysregulation is expected to play a significant role in esophageal cancer cell transformation. These data suggest that miR-185 alters cancer-associated pathway activity.

Although we used miR-16 as an internal control for the clinical evaluation of miR-185, a drawback is that endogenous sequences may not accurately reflect amplification of the

primary target owing to differences in primer sequence, the size of the amplified product, and the relative amounts of the two targets. Other internal controls are thus required for further confirmation. In addition, larger patient cohorts needs to be enlarged for future confirmation to predict prognosis.

References

1. Bray F, Ferlay J, Soerjomataram I, Siegel RL, Torre LA and Jemal A: Global cancer statistics 2018: GLOBOCAN estimates of incidence and mortality worldwide for 36 cancers in 185 countries. CA Cancer J Clin 68: 394-424, 2018.
2. Jin W, Luo W, Fang W, et al.: miR-145 expression level in tissue predicts prognosis of patients with esophageal squamous cell carcinoma. Pathol Res Pract 215: 152401, 2019.
3. Chen JG, Chen HZ, Zhu J, et al.: Cancer survival in patients from a hospital-based cancer registry, China. J Cancer 9: 851-860, 2018.
4. Rice TW, Ishwaran H, Hofstetter WL, et al.: Esophageal Cancer: Associations With (pN+) Lymph Node Metastases. Ann Surg 265: 122-129, 2017.
5. Skotland T, Sagini K, Sandvig K and Llorente A: An emerging focus on lipids in extracellular vesicles. Adv Drug Deliv Rev 159: 308-321, 2020.
6. Yang H, Fu H, Wang B, et al.: Exosomal miR-423-5p targets SUFU to promote cancer growth and metastasis and serves as a novel marker for gastric cancer. Mol Carcinog 57: 1223-1236, 2018.
7. Matsumoto Y, Kano M, Akutsu Y, et al.: Quantification of plasma exosome is a potential prognostic marker for esophageal squamous cell carcinoma. Oncol Rep 36: 2535-2543, 2016.
8. Matsumoto Y, Kano M, Murakami K, et al.: Tumor-derived exosomes influence the cell cycle and cell migration of human esophageal cancer cell lines. Cancer Sci 111: 4348-4358, 2020.
9. Fang P, Zhou J, Liang Z, et al.: Immunotherapy resistance in esophageal cancer: Possible mechanisms and clinical implications. Front Immunol 13: 975986, 2022.
10. Tang K, Toyozumi T, Murakami K, et al.: HIF-1α stimulates the progression of oesophageal squamous cell carcinoma by activating the Wnt/β-catenin signalling pathway. Br J Cancer 127: 474-487, 2022.
11. Berezikov E, Guryev V, van de Belt J, Wienholds E, Plasterk RH and Cuppen E: Phylogenetic shadowing and computational identification of human microRNA genes. Cell 120: 21-24, 2005.
12. Harada K, Baba Y, Ishimoto T, et al.: The role of microRNA in esophageal squamous cell carcinoma. J Gastroenterol 51: 520-530, 2016.
13. Niu Y and Tang G: miR-185-5p targets ROCK2 and inhibits cell migration and invasion of hepatocellular carcinoma. Oncol Lett 17: 5087-5093, 2019.

14. Liu C, Cai L and Li H: miR-185 regulates the growth of osteosarcoma cells via targeting Hexokinase 2. Mol Med Rep 20: 2774-2782, 2019.
15. Ostadrahimi S, Abedi Valugerdi M, Hassan M, et al.: miR-1266-5p and miR-185-5p Promote Cell Apoptosis in Human Prostate Cancer Cell Lines. Asian Pac J Cancer Prev 19: 2305-2311, 2018.
16. Zhang W, Sun Z, Su L, et al.: miRNA-185 serves as a prognostic factor and suppresses migration and invasion through Wnt1 in colon cancer. Eur J Pharmacol 825: 75-84, 2018.
17. Tan Z, Jiang H, Wu Y, et al.: miR-185 is an independent prognosis factor and suppresses tumor metastasis in gastric cancer. Mol Cell Biochem 386: 223-231, 2014.
18. Li BX, Yu Q, Shi ZL, Li P and Fu S: Circulating microRNAs in esophageal squamous cell carcinoma: association with locoregional staging and survival. Int J Clin Exp Med 8: 7241-7250, 2015.
19. Zhao ZT, Zhou W, Liu LY, Lan T, Zhan QM and Song YM: [Molecular mechanism and effect of microRNA185 on proliferation, migration and invasion of esophageal squamous cell carcinoma]. Zhonghua Yi Xue Za Zhi 93: 1426-1431, 2013.
20. Jing R, Chen W, Wang H, et al.: Plasma miR-185 is decreased in patients with esophageal squamous cell carcinoma and might suppress tumor migration and invasion by targeting RAGE. Am J Physiol Gastrointest Liver Physiol 309: G719-729, 2015.
21. Talukdar FR, di Pietro M, Secrier M, et al.: Molecular landscape of esophageal cancer: implications for early detection and personalized therapy. Ann N Y Acad Sci 1434: 342-359, 2018.
22. Zhang Y: Epidemiology of esophageal cancer. World J Gastroenterol 19: 5598-5606, 2013.
23. Manier S, Liu CJ, Avet-Loiseau H, et al.: Prognostic role of circulating exosomal miRNAs in multiple myeloma. Blood 129: 2429-2436, 2017.
24. Takeshita N, Hoshino I, Mori M, et al.: Serum microRNA expression profile: miR-1246 as a novel diagnostic and prognostic biomarker for oesophageal squamous cell carcinoma. Br J Cancer 108: 644-652, 2013.
25. Mercer TR and Mattick JS: Structure and function of long noncoding RNAs in epigenetic regulation. Nat Struct Mol Biol 20: 300-307, 2013.
26. Ge Q, Zhou Y, Lu J, Bai Y, Xie X and Lu Z: miRNA in plasma exosome is stable under different storage conditions. Molecules 19: 1568-1575, 2014.
27. Lu X and Kang Y: Hypoxia and hypoxia-inducible factors: master regulators of metastasis. Clin Cancer Res 16: 5928-5935, 2010.

28. Valeri N, Braconi C, Gasparini P, et al.: MicroRNA-135b promotes cancer progression by acting as a downstream effector of oncogenic pathways in colon cancer. Cancer Cell 25: 469-483, 2014.
29. Zhou W, Fong MY, Min Y, et al.: Cancer-secreted miR-105 destroys vascular endothelial barriers to promote metastasis. Cancer Cell 25: 501-515, 2014.
30. Garofalo M, Di Leva G, Romano G, et al.: miR-221&222 regulate TRAIL resistance and enhance tumorigenicity through PTEN and TIMP3 downregulation. Cancer Cell 16: 498-509, 2009.
31. Zhang Y, Yang P, Sun T, et al.: miR-126 and miR-126* repress recruitment of mesenchymal stem cells and inflammatory monocytes to inhibit breast cancer metastasis. Nat Cell Biol 15: 284-294, 2013.
32. Mao Y, Li L, Liu J, Wang L and Zhou Y: MiR-495 inhibits esophageal squamous cell carcinoma progression by targeting Akt1. Oncotarget 7: 51223-51236, 2016.
33. Zhao Y, Song Y, Yao L, Song G and Teng C: Circulating microRNAs: Promising Biomarkers Involved in Several Cancers and Other Diseases. DNA Cell Biol 36: 77-94, 2017.
34. Iorio MV and Croce CM: MicroRNAs in cancer: small molecules with a huge impact. J Clin Oncol 27: 5848-5856, 2009.
35. Xiang Y, Ma N, Wang D, et al.: MiR-152 and miR-185 co-contribute to ovarian cancer cells cisplatin sensitivity by targeting DNMT1 directly: a novel epigenetic therapy independent of decitabine. Oncogene 33: 378-386, 2014.
36. Fan L, Tan B, Li Y, et al.: Upregulation of miR-185 promotes apoptosis of the human gastric cancer cell line MGC803. Mol Med Rep 17: 3115-3122, 2018.
37. Değerli E, Torun V and Cansaran-Duman D: miR-185-5p response to usnic acid suppresses proliferation and regulating apoptosis in breast cancer cell by targeting Bcl2. Biol Res 53: 19, 2020.
38. Hassan M, Watari H, AbuAlmaaty A, Ohba Y and Sakuragi N: Apoptosis and molecular targeting therapy in cancer. Biomed Res Int 2014: 150845, 2014.

Figure 1

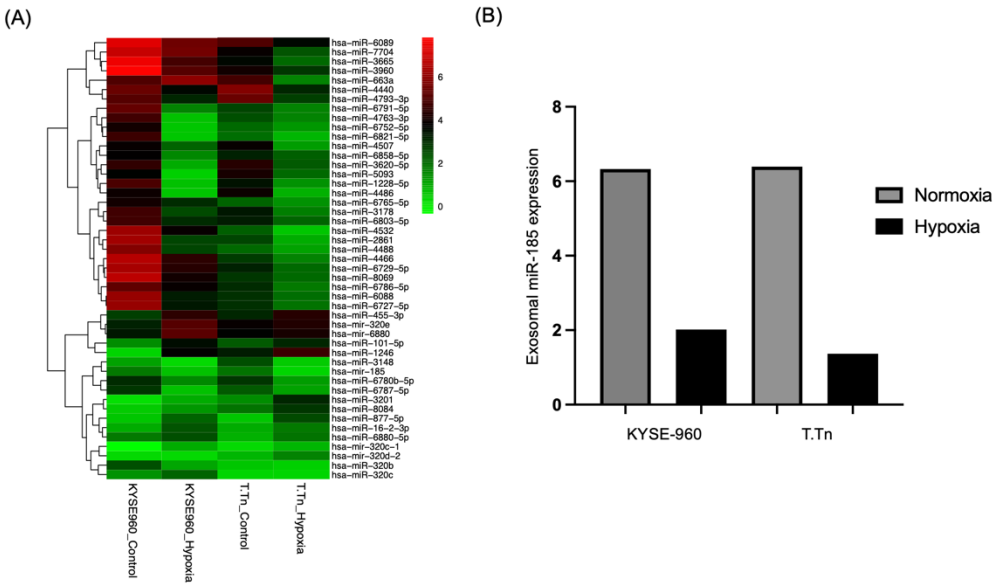

Figure 2

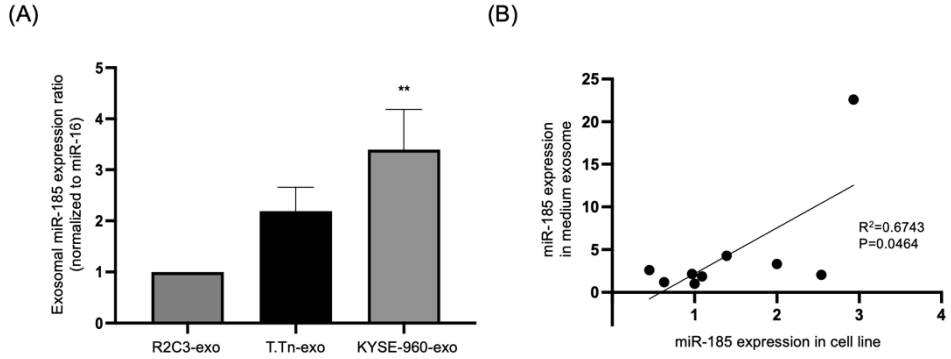

Figure 3

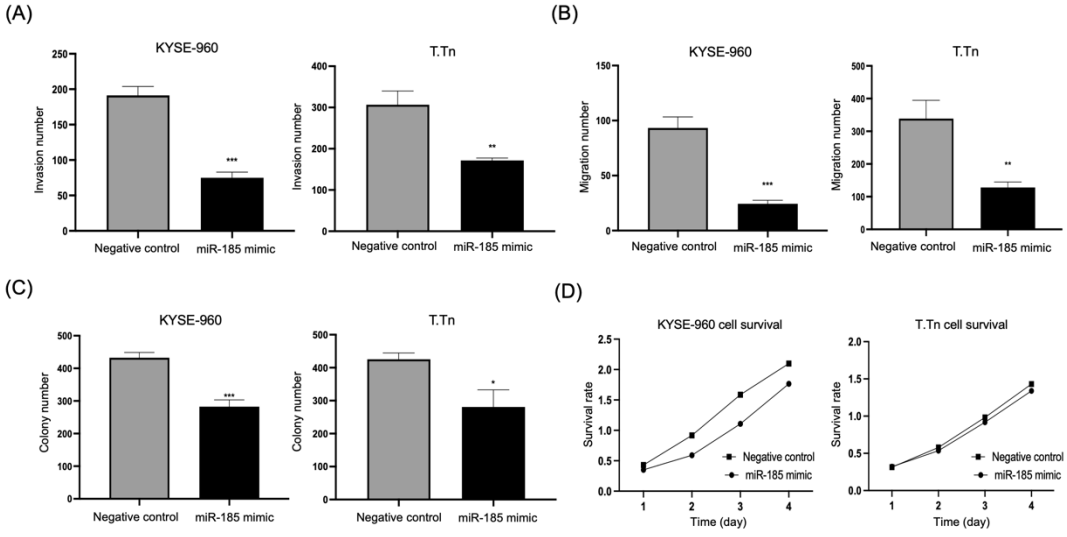

Figure 4

(A)

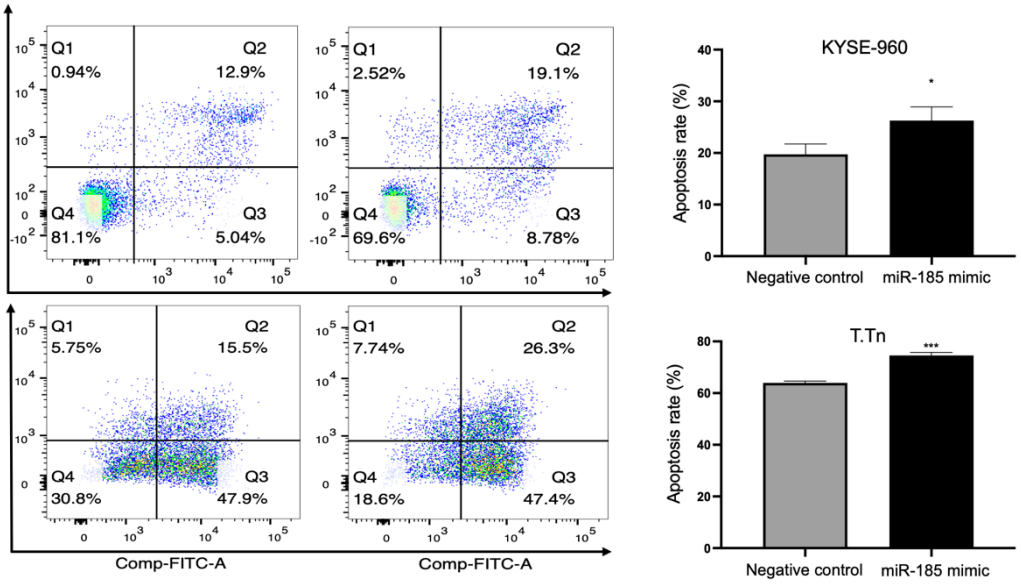

Figure 4

(B)

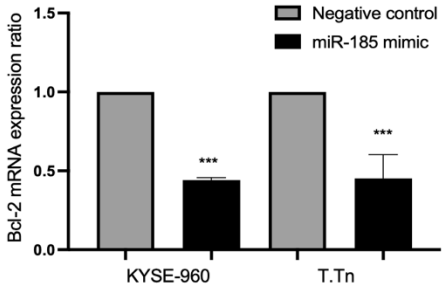

(C)

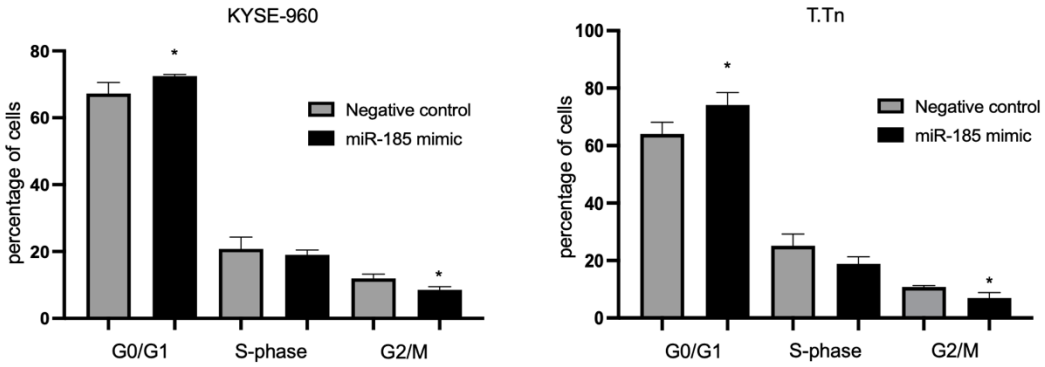

Figure 5 (A)

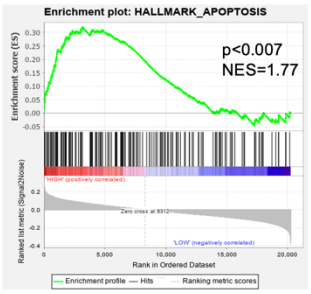

(B)

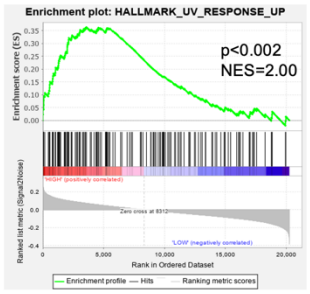

(C)

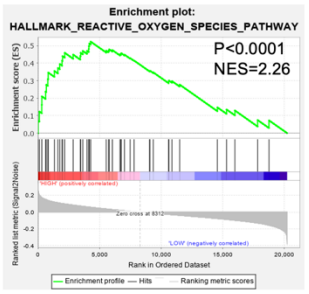

(D)

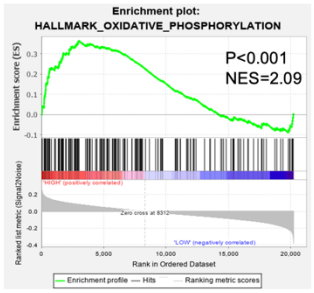

(E)

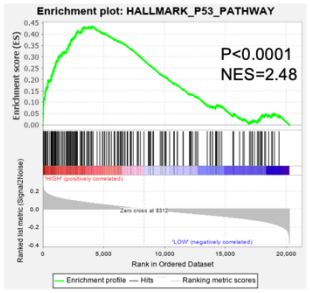

Figure 6

(A)

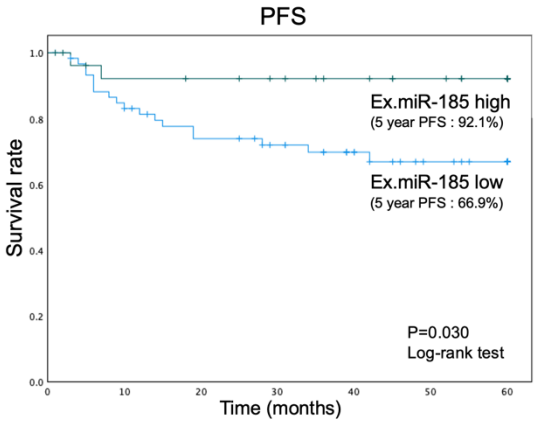

(B)

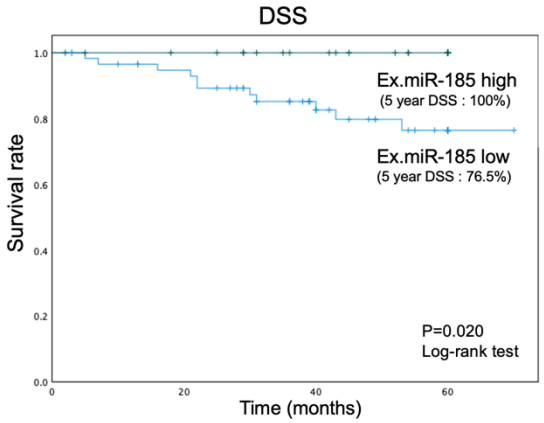

TABLE I. Demographics and clinicopathological characteristics in esophageal squamous cell carcinoma patients

Variables	Exosomal miR-185-5p high (n=28)	Exosomal miR-185-5p low (n=61)	P value
Mean age ± SD	66.6 ± 8.03	66.8 ± 8.32	0.923†
Sex, n			
Male/Female	24 / 4	51 / 10	1.000**
Histological Grade, n			
G1/G2/G3/X	4 / 15 / 7 / 2	11 / 29 / 13 / 8	0.853**
Location of the tumor			
Ce/Ut/Mt/Lt/Ae	0 / 2 / 15 / 10 / 1	0 / 8 / 27 / 23 / 3	0.836**
cT category, n			
cT1a+1b/2/3/4a+4b	16 / 7 / 5 / 0	25 / 15 / 21 / 0	0.235*
cN category, n			
cN0/1/2/3/4	20 / 2 / 3 / 0 / 3	28 / 11 / 18 / 4 /0	0.0045**
cM category, n			
cM0/1	28 / 0	61 / 0	1**
cStage, n			
cStage 0/1/2/3/4a/4b	7 / 6 / 9 / 3 / 3 /0	6 / 11 / 19 / 25 / 0/ 0	0.0001**
Treatment, n			
Endoscopic	6	3	0.0597**
Esophagectomy first	16	39	
NAC+Esophagectomy	6	19	
pT category, n			
pT0/1a+1b/2/3/4a	3 / 19 / 2 / 4 / 0	4 / 31 / 10 / 15 / 1	0.411**
pN category, n			
pN0/1/2/3/4/X	16 / 3 / 4 / 2 / 0 / 3	31 / 7 / 12 / 8 / 1 / 2	0.702**
pStage, n			
pStage 0/1/2/3/4a/X	2 / 11 / 5 / 5 / 2 / 3	1 / 18 / 14 / 15 / 9 / 4	0.527**

†Student t-test. *Chi-square test. ** Fisher's exact test.

TABLE II. Pathological response for NAC patients in esophageal squamous cell carcinoma

Variable	Exosomal miR-185-5p high (n=6)	Exosomal miR-185-5p low (n=19)	P value
Pathological response			
Grade 1a+1b/2/3	3 / 1 / 2	16 / 3 / 0	0.081**

** Fisher's exact test.

Figure S1

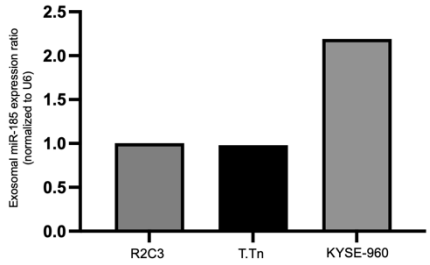

Figure S2

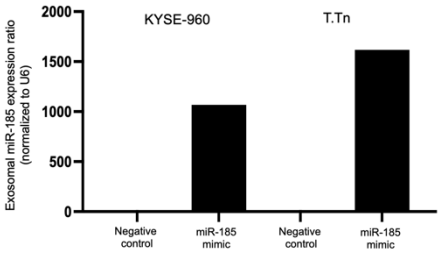

Figure S3

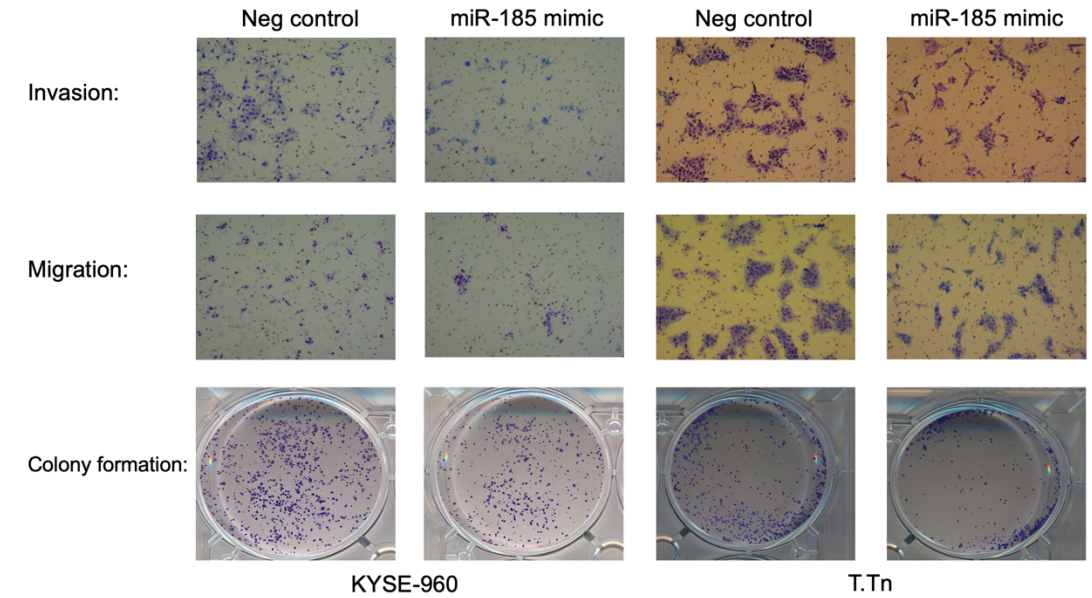

Figure S4

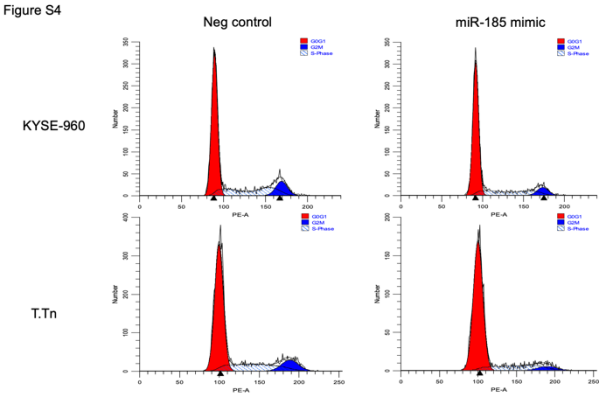

Figure S5

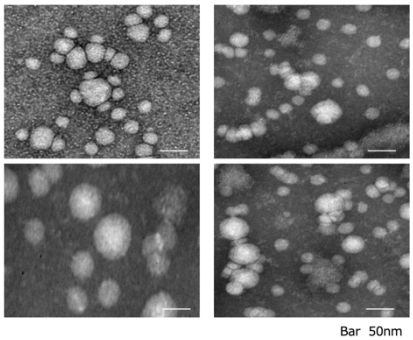

Figure Legends

Figure 1. (A) Hierarchical clustering of the differentially expressed miRNAs in ESCC cell lines culture medium. Hypoxia affects miRNA expression in KYSE-960 and T.Tn cell culture medium. Differentially regulated miRNAs were hierarchically clustered. In the KYSE-960 cell line, 33 miRNAs were downregulated and 12 were upregulated. In T.Tn cell lines, 33 miRNAs were downregulated and 9 were upregulated. The intensity represents the magnitude of expression difference. Expression levels of miRNAs that are two-fold upregulated (red) or downregulated (green) in normoxic and hypoxic cells are displayed through heatmaps. The expression values are log-transformed. (B) Exosomal miR-185 expression is downregulated in both KYSE-960 and T.Tn cell line culture medium (KYSE-960 fold-change: 0.32, T.Tn fold-change: 0.22).

Figure 2. (A) R2C3, T.Tn, and KYSE-960 were cultured in exosome-free medium, and miR-185 expression was measured via qRT–PCR. MiR-16 was used as an internal control; $p = 0.075$, $^{**}p = 0.0036$. (B) Correlation analysis of miR-185 expression in exosomes from cancer cell medium and cell lines, quantified via qRT–PCR ($r^2 = 0.6743$, $p = 0.0464$).

Figure 3. (A, B) Transwell assays were used to detect cell migration and invasion abilities of KYSE-960 and T.Tn cells after transfection. (invasion: $^{***}p < 0.0003$, $^{**}p < 0.003$; migration: $^{***}P < 0.0004$, $^{***}P < 0.0002$). (C) Colony formation assays were performed to assess the colony formation ability of KYSE-960 and T.Tn cells ($^{***}p < 0.0005$: $^{*}p < 0.01$). (D) CCK-8 assays were used to detect the viability of KYSE-960 and T.Tn cells after transfection ($^{**}p < 0.002$, $p < 0.6$).

Figure 4. (A) Cell apoptosis was evaluated through FACS with Annexin V-FITC and propidium iodine staining. (B) qRT–PCR was used to the detect mRNA expression of BCL-2 in KYSE-960 and T.Tn cell lines. β-actin gene was used a housekeeping gene ($p < 0.0009$; $p < 0.00002$). (C) For the cell cycle analyses, the histogram is plotted for changes in cell cycle progression in each group.

Figure 5. Gene set enrichment analysis (GSEA) was used to analyze the signaling pathways enriched in different groups: (A) apoptosis, (B) UV response, (C) reactive oxygen species pathway, (D) oxidative phosphorylation, (E) p53 pathway. Normalized

enrichment score (NES) indicated the extent of enrichment per gene sets. False discovery rate (FDR) indicated the significance of enrichment. ES, enrichment score. Gene sets for enrichment analysis were determined based on adjusted *p*-value (< 0.05) and normalized enrichment score (|NES| > 1).

Figure 6. Kaplan–Meier survival curves showing the relationship between high or low plasma exosomal miR-185-5p levels with (A) progression-free survival (PFS) and (B) disease-specific survival (DSS) of patients with esophageal squamous cell carcinoma.

Tables

Table 1. Demographics and clinicopathological characteristics in esophageal squamous cell carcinoma patients

Patients were divided into circulating miR-185-high (n = 28) and -low (n = 61) groups. A cutoff value was set for the miR-185/miR-16 ratio based on the mean value of miR-185 in esophageal cancer patients. In patients with high circulating exosomal miR-185, the frequency of lymph node metastasis in the preoperative diagnosis was significantly lower (p = 0.0045), as was the cStage (p = 0.0001). †Student's t-test, *Chi-square test. ** Fisher's exact test.

Table 2. Pathological response of NAC patients with esophageal squamous cell carcinoma

The preoperative patient group with high circulating exosomal miR-185 (n = 6) tended to exhibit a slightly higher response rate to chemotherapy than patients with low circulating exosomal miR-185 (n = 19) [p = 0.081]. ** Fisher's exact test.

Supplementary materials

Figure S1. Expression of miR-185 in normal esophageal keratinocytes (R2C3) and esophageal cancer cell lines (T.Tn and KYSE-960).

Figure S2. qRT–PCR of miR-185 expression in KYSE-960 and T.Tn cells transfected with miR-185 or a negative control. The expression value of miR-185 in the negative control groups was confirmed as 1 compared to KYSE-960 and T.Tn mimic groups.

Figure S3. The diagram of invasion, migration, and colony formation.

Figure S4. The diagram of flow cytometric analysis of cell cycle.

Figure S5. Exosome isolation from plasma was confirmed via transmission electron microscopy. (Bar: 50 nm)

Table S1. Primer sequences used for qRT–PCR.

Oncology Letters vol.28 No.1
2024 年 5 月 22 日　　公表済
DOI：10.3892/ol.2024.14467